Modelling the partitioning of turbulent fluxes at urban sites with varying vegetation cover

Article

Accepted Version

It is advisable to refer to the publisher's version if you intend to cite from the work. See Guidance on citing.

To link to this article DOI: http://dx.doi.org/10.1175/JHM-D-15-0126.1

Publisher: American Meteorological Society

www.reading.ac.uk/centaur

CentAUR

Central Archive at the University of Reading

Reading's research outputs online

Modelling the partitioning of turbulent fluxes at urban sites with varying vegetation cover

MJ Best [1,2], CSB Grimmond [2,3]

[1] Met Office, FitzRoy Road, Exeter, EX1 3PB, UK [2] King's College London, Department of Geography, London, WC2R 2LS, UK
[3] Department of Meteorology, University of Reading, Earley Gate, PO Box 243, Reading, RG6 6BB, UK

Abstract: *Inclusion of vegetation is critical for urban land surface models (ULSM) to represent reasonably the turbulent sensible and latent heat flux densities in an urban environment. Here the Joint UK Land Environment Simulator (JULES), an ULSM, is used to simulate the Bowen ratio at a number of urban and rural sites with vegetation cover varying between 1% and 98%. The results show that JULES is able to represent the observed Bowen ratios, but only when the additional anthropogenic water supplied into the urban ecosystem is considered. The impact of the external water use (irrigation, street cleaning), for example, on the surface energy flux partitioning can be as substantial as that of the anthropogenic heat flux on the sensible and latent heat fluxes. The Bowen ratio varies from 1-2 when the plan area vegetation fraction is between 30% and 70%. However, when the vegetation fraction is less than 20%, the Bowen ratios increase substantially (2-10) and have greater sensitivity to assumptions about external water use. As there are few long term observational sites with vegetation cover less than 30%, there is a clear need for more measurement studies in such environments.*
Key Words: Bowen ratio, irrigation, JULES, land surface model, spin-up strategy, urban vegetation

1. Introduction

Over the last couple of decades a number of models have been developed to represent urban land-surface-atmosphere interactions, such as the Building Effect Parameteriztion (BEP, Martilli et al., 2002), Slab urban energy balance model (Fortuniak, 2003), Multilayer urban canopy model (Kondo et al., 2005), Community Land Model – urban (CLM-urban, Oleson et al., 2008), and the Seoul National University urban canopy model (Ryu et al., 2011). Typically these models are designed to represent the energy balance of the various facets that make up an idealized urban canopy. Often this idealized urban canopy is treated as a symmetric street canyon geometry with varying degrees of complexity, ranging from a bulk canyon (e.g., Best, 2005), separate roof, walls and road, with single (e.g., Masson, 2000) or multiple (e.g., Krayenhoff and Voogt, 2007) energy balances, and even intersections separate from street canyons (e.g., Kawai et al., 2009). Whilst this may be a good representation of the central downtown areas of major cities, this design alone (i.e., without a representation of vegetation) does not capture the influence of vegetation present in many street canyons and abundant in the suburbs of many cities.

The implications are that vegetation also needs to be modelled for urban areas. Indeed, the first international urban model comparison experiment (PILPS-Urban) concluded that for the two urban sites considered in the study (Vancouver and Melbourne), models that included a representation of vegetation performed much better in simulating the sensible (Q_H) and latent heat (Q_E) densities than models that neglected it (Grimmond et al., 2010, 2011, Best and Grimmond, 2013, 2015a). PILPS-Urban also concluded that the way in which the vegetation was modelled, i.e., as a separate independent surface (e.g., Dupont and Mestayer, 2006) or integrated within the urban street canyon (e.g., Lee and Park, 2008) was not as important. However, the main focus of PILPS-Urban results was a suburban site, so it is not clear how robust these conclusions are for other sites with varying fractions of vegetation within the footprint of the observations.

Observational data have quantified directly Q_H and Q_E and hence how the Bowen Ratio β (i.e., $\beta = Q_H/Q_E$) varies with the vegetation fraction across a range of values (Grimmond and Oke, 2002, Loridan and Grimmond, 2012a). Here we investigate if an urban model that includes a representation of vegetation can reproduce this observed behaviour.

In this study we use the JULES model (Best et al., 2011). It has been shown to perform well in simulating Q_H and Q_E compared to other models within PILPS-Urban (Best and Grimmond, 2015b). Here the model is used to simulate β for urban areas that range in plan area vegetation cover (i.e., two-dimensional vegetation cover as viewed from above) from 1% to 98%, that correspond to 22 observational dataset footprint descriptions.

2. Methods
2.1 Observational sites

For this modelling study, evaluation data come from 22 observational tower sites (Table 1) where Q_H and Q_E were measured by eddy covariance in the inertial sublayer above usually uniform urban canopies. The measurements represent the neighborhood or local scale surface energy balance. The methods and analysis techniques used at each site are described in the papers corresponding to the individual sites (Table 1). The datasets include both short (< two months) and long (> 12 months) durations, with the longest (Baltimore) spanning six years. Most of the shorter datasets were collected in the summer months. For mid-latitudes and semi-arid climates, the summer months are the periods during which the vegetation is most likely to experience soil moisture stress and hence limited transpiration. The datasets with observations collected during the winter (Ouagadougou and Mexico City) are sub-tropical climates where the precipitation is typically less during the winter months. Hence these are also the periods that are more likely to have

soil moisture stress on the vegetation. Two rural sites outside of Basel (R1 and R2) were added to complete the spectrum of vegetation cover fractions modelled.

The surface characteristics affecting the measurements have a range in vegetation cover amounts from almost full vegetation cover to only 1% (Table 2). The surface cover data used in this study are from the literature. For the few sites with only the total vegetation amount reported, additional analyses were undertaken of available satellite imagery to subdivide this further.

For most of the sites the plan area proportions of vegetation and impervious surfaces (streets and buildings) combine to account for around 95% of the total area, with the exceptions of Tucson and Ouagadougou. These two sites have substantial areas of bare soil or unmanaged land (17% and 30% respectively, which is modelled as bare soil). However, both these sites are in relatively dry climates and so bare soil evaporation is unlikely to have a substantial contribution to Q_E, and hence β.

Forcing data for urban land surface models typically includes the downward components of both shortwave and longwave radiation, precipitation, surface pressure and near surface atmospheric wind, temperature, and humidity. Details on the observation of each of these variables at each of the measurement sites can be found in the references provided in Table 1. For many of the earlier datasets, the radiation components were not observed at the sites, but have been taken from nearby observational stations that make routine measurements, or derived from empirical formulae.

Table 1: Sources of observational data used in the analyses, with the main references for the data and the site characteristics.

City	Site name	LCZ[a]	Lat / Long	Period / Length	Data averaging period (mins)	Instrument height (m)	References
Arcadia, CA, USA	Arcadia (93)	8	34.1° N 118.0° W	Jul - Aug 93 40 days	60	30.5	Grimmond and Oke, 1995 Grimmond and Oke, 2002
Arcadia, CA, USA	Arcadia (94)	6	34.1° N 118.0° W	Jul 94 19 days	60	32.8	Grimmond et al., 1996 Grimmond and Oke, 2002
Baltimore, MD, USA	Baltimore	6	39.2° N 76.7° W	May 01 – Dec 06 2049 days	60	41.2	Crawford et al., 2011 Loridan et al., 2011
Basel, Switzerland: Grenzach Village Neuf, Allschwil, Sperrstrasse, Spalenring,	Basel (R1) Basel (R2) Basel (S1) Basel (U1) Basel (U2)	D D 6 2 2	47.5° N 7.7° E	Jun – Jul 02 30 days	10	1.5 – 28.0 2.0 – 3.3 15.0 – 15.8 25.5 – 31.7 33.0 – 37.6	Christen and Vogt, 2004
Chicago, IL, USA	Chicago (92)	6	41.6° N 87.5° W	Jul 92 13 days	60	18.0	Grimmond and Oke, 1995 Grimmond and Oke, 2002
Chicago, IL, USA	Chicago (95)	6	41.6° N 87.5° W	Jun - Aug 95 57 days	60	27.0	King and Grimmond, 1997 Grimmond and Oke, 2002
Helsinki, Finland	Helsinki	mixed	60.2° N 24.9° E	Sep 07 - Dec 09 853 days	30	31.0	Vesala et al., 2008 Jarvi et al., 2014
Lodz, Poland	Lodz	2	51.8° N 19.5° E	Mar 01 - Dec 02 730 days	60	37.0	Offerle et al., 2005a, 2006a, 2006b Pawlak et al., 2011
Marseille, France	Marseille	2	43.2° N 5.2° E	Jun - Jul 01 27 days	60	39.0	Grimmond et al., 2004
Melbourne, Australia	Melbourne	6	37.8° S 144.9° E	Aug 03 – Nov 04 475 days	30	35.0	Coutts et al., 2007a Coutts et al, 2007b
Mexico City, Mexico	Mexico City	2	19.2° N 99.1° E	Dec 93 7 days	60	28.0	Oke et al., 1999 Grimmond and Oke, 2002
Miami, FL, USA	Miami	6	25.4° N 80.2° W	May - Jun 95 26 days	60	40.8	Newton, 1999 Grimmond and Oke, 2002 Newton et al., 2007
Ouagadougou, Burkina Faso	Ouagadougou	Not classified	12.2° N 1.3° E	Feb 03 26 days	60	10.0	Offerle et al., 2005b
San Gabriel, CA, USA	San Gabriel	3	34.1° N 118.0° W	Jul 94 22 days	60	18.0	Grimmond et al., 1996 Grimmond and Oke, 2002
Sacramento, CA, USA	Sacramento	6	38.3° N 121.3° W	Aug 91 10 days	60	29.0	Grimmond et al., 1993 Grimmond and Oke, 1995 Grimmond and Oke, 1999 Grimmond and Oke, 2002
Tucson, AZ, USA	Tucson	7	32.1° N 110.6° W	May – Jun 90 45 days	60	25.6	Grimmond and Oke, 1995 Grimmond and Oke, 2002
Vancouver, Canada	Vancouver (L92)	8	49.3° N 123.1° W	Aug 92 15 days	60	9.0	Grimmond and Oke, 1999 Grimmond and Oke, 2002
Vancouver, Canada	Vancouver (S92)	6	49.3° N 123.1° W	Jul - Sep 92 56 days	60	14.1	Grimmond and Oke, 1999 Grimmond and Oke, 2002

[a] Local climate zones according to Stewart and Oke (2012) as published in Grimmond and Christen (2012).

Table 2: Sites ordered by increasing plan area cover of vegetation within the observational footprint. See Table 1 for site names and sources of data. * indicates the sites where judgement had to be used to determine tree and grass cover.

Site	Site code[b]	Trees (%)	Grass (%)	Total Veg (%)	Buildings (%)	Streets (%)	Total built (%)	Bare soil (%)	Water (%)
Mexico City	Me93	1	0	**1**	54	44	97	2	0
Vancouver (VL92)	Vl92	3	2	**5**	51	44	95	0	0
Ouagadougou	Oa03	10	0	**10**	40	20	60	30	0
Marseille	Ma01	13	0	**13**	60	27	86	1	0
Basel (U1)	Ba02u1	11 *	5 *	**16**	54	30	84	0	0
Tucson	Tu90u	11	7	**18**	23	42	65	17	0
Lodz	Lo06[c]	22 *	9 *	**31**	30	40	69	0	0
Basel (U2)	Ba02u2	16 *	15 *	**31**	37	32	69	0	0
Miami	Mi95	7	27	**34**	35	29	64	0	2
San Gabriel	Sg94	12	25	**37**	29	31	60	0	4
Melbourne	Mb03m	23	15	**38**	45	18	62	1	0
Chicago (95)	Ch95	7	32	**39**	36	25	61	0	0
Vancouver (VS92)	Va08s[C]	9	35	**44**	31	24	55	2	0
Chicago (92)	Ch92	10	34	**44**	33	22	55	1	0
Sacramento	Sc91u	13	34	**47**	36	12	48	1	5
Helsinki	He05	24	25	**49**	15	36	51	0	0
Arcadia (94)	Ar94	30	23	**53**	24	19	43	2	2
Basel (S1)	Ba02s1	21 *	32 *	**53**	28	19	47	0	0
Arcadia (93)	Ar93	32	24	**56**	22	18	40	2	2
Baltimore	Bm02	54	14	**67**	16	15	31	1	1
Basel (R1)	-	9 *	82 *	**91**	2	7	9	0	0
Basel (R2)	-	0 *	98 *	**98**	0	2	2	0	0

[b] Site code as published in Grimmond and Christen (2012). [c] There are multiple observational datasets for the same site.

2.2 Gap-filling for forcing data

As forcing data need to be continuous to undertake the simulations, any observational gaps need to be filled. For this study, the processed gap-filled forcing data from Loridan and Grimmond (2012b) are used where available. At sites where these processed data were not available, further gap-filling of the original observational datasets is required. Whilst short periods (a few data values) can be filled using simple interpolation methods, this is not possible for longer periods. Hence an alternative method is required.

For this current study, data from the WFDEI (WATCH Forcing Data methodology applied to ERA-Interim reanalysis data, Weedon et al., 2011, 2014) dataset have been used to fill any missing data gaps in the observational dataset. WFDEI spans the period from 1979 to 2012 and includes the data required to force land surface models. The dataset is global at 0.5° spatial resolution and has been derived using ERA-Interim re-analyses (Dee et al., 2011) to downscale monthly observations from the Climate Research Unit (CRU, New et al. 1999, 2000, Harris et al., 2013) to a temporal resolution of three hours (see Weedon et al., 2011, 2014, for more details). For precipitation, WFDEI has an alternative that is derived from the Global Precipitation Climatology Centre (GPCC, Schneider et al., 2013) for the monthly observations rather than CRU. In this study the WFDEI dataset based on GPCC precipitation are used.

Given the global gridded nature of the WFDEI data (Weedon et al., 2011, 2014) it is quite likely that there are inconsistencies between these data and those observed at the study sites. In particular, the long term grid mean of WFDEI may not match a specific observational site mean. To asses this, periods with values in the observational dataset for the sites were used to determine if any biases existed in the WFDEI data. Any bias found was then applied to the WFDEI data to create values that could be used to gap-fill the observational dataset whilst maintaining a consistent mean state.

Whilst the forcing data are gap-filled, the observations used to evaluate the models is restricted to periods with valid observational data.

2.3 Model description

The model used for this study was the community land surface model JULES (Joint UK Land Environment Simulator, Best et al., 2011). This model uses a tiled approach to represent surface heterogeneity in land cover and by default includes five types of vegetation (two types of trees, two types of grasses and shrubs) and four non-vegetation types (urban, lakes, bare soil and permanent land ice), for which the urban tile represents the impervious surfaces of an urban environment.

This model has an aerodynamic resistance formulation based upon Monin-Obukhov similarity theory (Monin and Obukhov, 1954), whilst the resistance for surface water comes from either a simple water holding capacity for non-vegetation surfaces, or stomatal resistance for vegetation based upon the photosynthesis model of Collatz et al. (1991, 1992). For vegetation, water is extracted from the soil based upon an exponential rooting depth profile, with the e-folding depth (the depth of soil that contains the fraction $(1-e^{-1})$ of the roots) dependent on vegetation type. Trees have a rooting depth profile that primarily has roots in the bottom most layers, whereas grasses have roots that are primarily in the top soil layers. The leaf area index (LAI) for vegetated surfaces can vary temporally, but for this study they have been held fixed at their default values for all sites (Best et al., 2011).

Water infiltration into the soil is determined by the saturated hydraulic conductivity of the soil, with an additional enhancement factor that varies between vegetation types (Best et al., 2011). The soil is treated as a one dimensional vertical column and is solved using a finite difference form of the Richards equation (Best et al., 2011). The thermal structure of the soil is modeled using the diffusion equation, and the energy equations include the vertical transport of the soil moisture along with phase changes of the water. The soil processes for both heat and water are modelled using the same four discrete layers and have increasing thickness with depth, the layer depths being 0.1 m, 0.35 m, 1.0 m and 2.0 m, respectively. The bottom boundary conditions for the soil are free drainage and a zero heat flux for energy conservation.

Results from the PLUMBER (PALS Land sUrface Model Benchmarking Evaluation pRoject) community experiment showed the performance of this model for Q_H and Q_E, at a number of sites with natural surfaces, is comparable to many other land surface models (LSM) (Best et al., 2015).

Within this model there are three ways in which the impervious urban surface (i.e., ground (e.g., roads, parking lots) and buildings, excluding the vegetation and bare soil) can be represented, namely the one tile (Best, 2005), two tile (Best et al., 2006) and MORUSES (Porson et al., 2010) schemes. The one tile scheme represents an urban area as a bulk surface with parameters that represent a block of concrete. The two tile scheme separates out the roofs of buildings from the street canyon, but the parameters for each surface are held constant and thus do not vary in space or time. The MORUSES scheme is similar to the two tile scheme except that the parameters and canyon turbulence is parametrised and depends upon the morphology of the urban area.

Results for all three versions were included in PILPS-urban, although MORUSES was an early version that did not include vegetation. Results from the one tile and two tile versions of JULES were submitted by two modelling groups with different assumptions about their initial conditions of soil moisture. Results presented in Best and Grimmond (2014) showed that the initial conditions for soil moisture can have a substantial impact on Q_H and Q_E. However, Best and Grimmond (2015b) show that four applications of JULES (a one tile and a two tile version run by two modelling groups) performed well in simulating Q_H and Q_E compared to other models in PILPS-Urban. For this study we have chosen to use solely the two tile urban scheme within JULES, because Best et al. (2006) showed that this performed better than the one tile version, but have ensured that the initial conditions for the runs are appropriate by undertaking a spin-up simulation, as described below.

2.4 Spin-up strategy.

Analysis of the results from PILPS-Urban showed that the initial conditions of soil moisture are important for the correct evolution of Q_H and Q_E (Best and Grimmond, 2014). In addition,
initial preparation work for the PLUMBER community benchmarking experiment (Best et al., 2015) identified that a 10 year spin-up period for soil moisture was sufficient provided the initial soil moisture was set to saturation, because gravitational drainage helps to remove excess water. However, if the soil moisture was set too dry before the spin-up, then a 10 year period was not sufficient for all climates.

A common method to spin-up the soil moisture is to repeat the first year of the simulation repeatedly (e.g., 10 times). However, this results in soil moisture that is in equilibrium with the climatic conditions of the selected year and not necessarily a representative soil moisture that would have evolved from the climate prior to the study period. As many of the observational datasets considered in this study are shorter than a year, this method cannot be applied. Therefore, to be consistent between sites, an extended atmospheric forcing dataset (at least 10 years) prior to the period of the observational study for all study sites was extracted from the WFDEI dataset used for gap-filling the forcing data (section 2.2).

For each site the extracted WFDEI grid data were used to force JULES with a 30 min time-step. The temporal interpolation from the three hour resolution of WFDEI used a simplified Sheng and Zwiers (1998) algorithm within JULES. For radiation and precipitation data, a backward time averaging (i.e., time averaging that is valid at the end of the time period) that conserves the mean quantity is used, whilst for the other forcing variables a linear interpolation is used. The WFDEI temperature and humidity data are provided at screen level whilst the wind data are at 10 m height. However, the surface of the JULES model is not the true surface, but one that incorporates the displacement height (i.e.,

the displacement height is not explicitly represented), so the WFDEI data have been used to force the model without any changes to the height. This is acceptable because the spin-up only needs to be in agreement with the previous mean climate, which can still be obtained from forcing at the heights of the WFDEI data.

Hence for each observational site (Table 1) JULES was run for at least 10 years prior to the initial period of the observational study, forced with atmospheric data from WFDEI. The soil moisture state at the beginning of the spin-up was specified as being saturated conditions. The LSM was then run for the entire period to try to ensure that the soil moisture reaches a correctly spun-up state. The soil moisture at the end of the spin-up period provides the initial conditions of soil moisture at the start of the analysis period. The results from the analysis period are then taken from the continuous model simulation forced by the gap-filled data from the observations at the study sites, with the length of the model integration determined by the length of the observational dataset, which varied from 7 to 2049 days (Table 1).

2.5 Model simulations

Land cover fractions were determined from publications about the sites (Table 2). For most the tree cover was separate from grass, but broadleaf or needle-leaf were not specified. For the current study it was assumed that trees were broadleaf and that the grass fraction was lawn.

Values of Q_H and Q_E from the model simulations were used to derive β around mid-day, based on the average of each flux density between hours ending 10:00 and 14:00 local solar time (LST) on each day:

$$\overline{X} = \sum_{i=1}^{N_{days}} \sum_{j=10}^{14} X_{ij}$$

where X represents Q_H or Q_E, X_{ij} is the flux density at time j ($10:00 \leq j \leq 14:00$) on day i of the N_{days} of the simulation, and $\overline{X}$ is the mid-day average. The long term Bowen Ratio (β) is the ratio of the averaged flux densities:

$$\beta = \frac{\overline{Q_H}}{\overline{Q_E}}$$

and was defined the same way for both the observations and model results, with missing observations periods omitted from both calculations. A mid-day value for β was used in preference to a daily average value because both fluxes are likely to be positive during the mid-day period, and Q_E (the denominator of β) is not usually close to zero, making the Bowen ratio more meaningful.

There could be many sources of errors in the model simulation that could impact on all of the terms within the surface energy balance, such as incorrect surface albedos and unknown thermal heat storage properties of the building materials. Here the focus is the ability of the model to partition the surface fluxes between turbulent heat and moisture, hence β, and not the individual flux densities.

3 Results and discussion

Although the 18 short duration datasets cannot be analysed for seasonal variations, it is possible with the four multi-year datasets (Baltimore, Helsinki, Lodz and Melbourne, see Table 1). However, as the results for each season are consistent with those for all available data (not shown), the analyses presented use all available data at each site.

Fig. 1: Mid-day (10:00 – 14:00 local solar time) variability of observed and modelled Bowen ratio (β) shown with the inter-quartile range (box), median (-) and 10th and 90th percentiles (whiskers).

The observed and modelled β values for each of the sites are shown in Fig. 1. The model results are in good agreement with observed β at a number of the sites (e.g., the two urban sites in Basel (U1, U2), Miami, Chicago (95), see Table 1 for sites), but at the majority of the sites β is overestimated by the model. At only one site is β substantially lower than the observed value (Vancouver (VS92)). If β is too large, this implies that modelled Q_H is too large compared to Q_E, whilst a value that is too small implies that modelled Q_E is too large compared to Q_H.
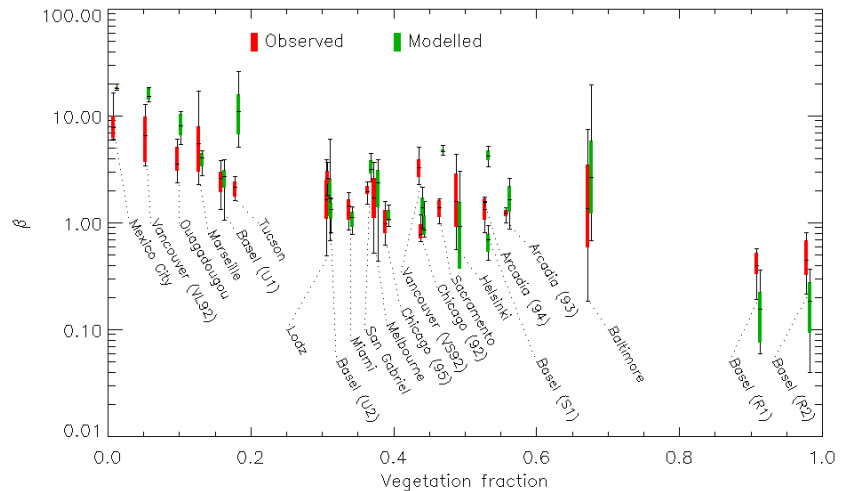
In the following discussion we highlight cases where JULES simulations and measurements disagree to explore further possible model improvements.

3.1 Influence of garden irrigation

One possible explanation for large β values in the JULES model is that the vegetation could be soil moisture stressed, and hence the transpiration has been reduced. To investigate the potential impact of the soil moisture, Figure 2 shows the initial soil moisture profile (after the model spin-up) within the soil column normalised by the critical point (the point at which vegetation starts to become soil moisture stressed within JULES, Best et al., 2011). A value less than one for any layer indicates that there is reduced soil moisture available to the roots in that layer, which will thus restrict the transpiration accordingly.

Different root density profiles are used within JULES which correspond to where soil moisture may be removed from by trees and grass (Fig. 2). For grass, soil moisture can be removed primarily from the second and third soil layers (0.1 - 1.0 m depth) within the model, whilst for trees the third and fourth soil layers (0.35 - 3.0 m depth) are the primary sources.

For many of the sites for which the model over predicts β (Tucson, Melbourne, Sacramento, Arcadia (94), San Gabriel, Arcadia (93), Ouagadougou, Fig. 1), the initial soil moisture profile (Fig. 2) was below the critical point for at least two of the four soil layers within the model.

Fig. 2: Initial soil moisture profile used in the model simulations at each site (Table 1) derived from the spin-up, and the model root density profiles for a grass and tree land cover type. Horizontal dashed lines show the soil level boundaries.
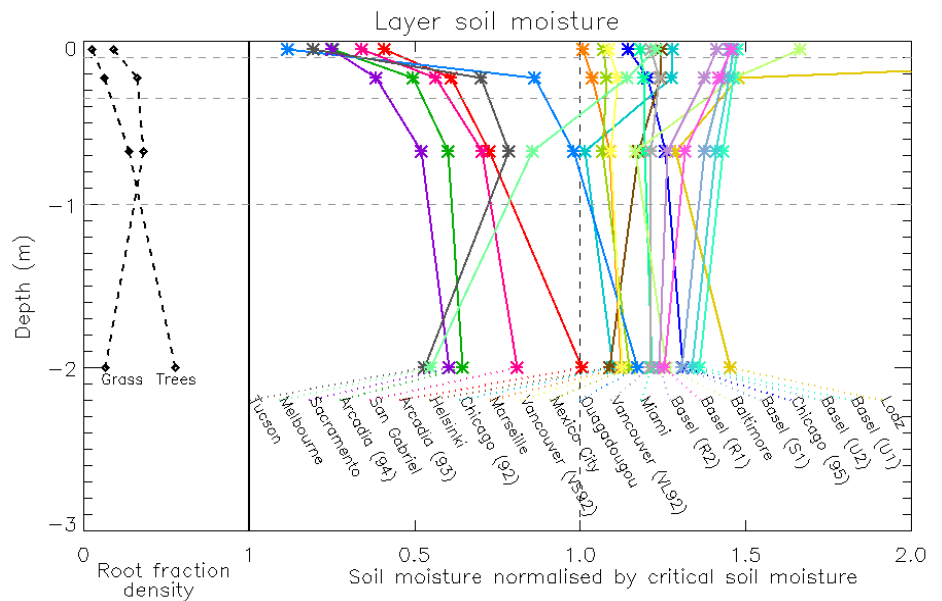
The JULES model does not have a representation of irrigation. So to investigate the impact of the soil moisture stress on the vegetation, the model was re-run for each site, but with the unfrozen soil moisture (i.e., the liquid water phase that is available for transpiration) in every layer set to the critical point (or saturation minus frozen soil moisture if this was smaller) at each time-step, i.e., no soil moisture stress for the vegetation. This can be thought of as 'optimal irrigation', equivalent to the minimum irrigation required to ensure that transpiration from the vegetation has no soil moisture limitation. The results of these simulations are shown in Fig. 3, along with the original default JULES simulations. Maintaining the soil moisture at the critical point in each layer reduces β to below that of the observations for most of the sites. Hence the model can represent observed β values, but only if there is no soil moisture stress for the vegetation.

Fig. 3: as for Fig.1, Observed and JULES model runs: initial/Default, and with irrigation. Irrigation amount is based on model soil moisture fixed at the critical point. See text for further discussion. Sites are organised by increasing plan area fraction vegetated (see Table 2 for values).
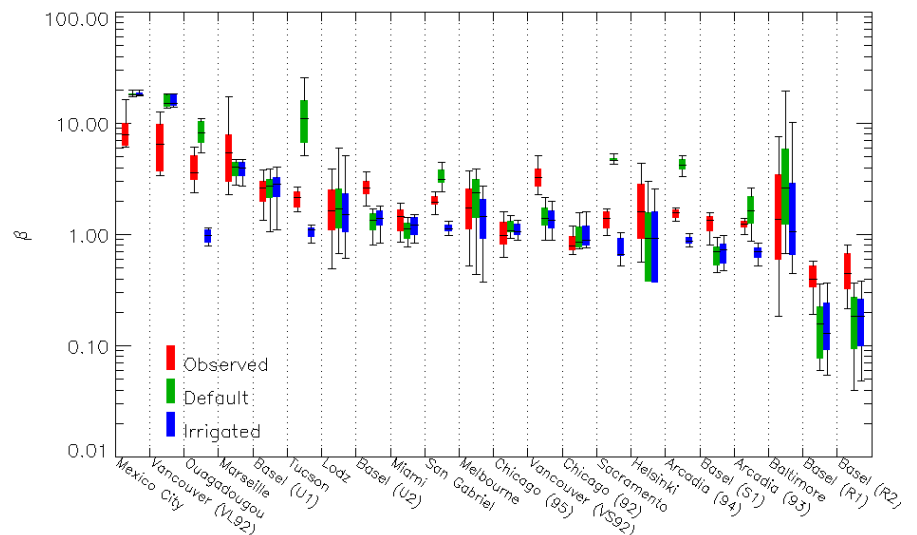
The spin-up strategy (section 2.4) used to initialise the soil moisture for each of the sites should have resulted in a reasonable initial state, based upon knowledge resulting from previous work (Best et al., 2015). However, for the work of Best et al. (2015) there were no anthropogenic influences at

the study sites. At the urban sites of interest here, the additional soil moisture required to give a good simulation from the model could be the absence of an anthropogenic water injection. This may be watering by individuals to maintain their gardens (e.g., Sacramento) or street cleaning by the city to clear up after markets (e.g., Mexico City, Marseille). Such additions of anthropogenic water may also be regulated; for example, irrigation on alternating days (odd/even) such as Sacramento (Grimmond and Oke, 2002) or banned such as Vancouver (VS92) because of drought. Under unrestricted irrigation conditions, Q_E closely follows irrigation (Grimmond and Oke 1986). Given the watering of gardens is to ensure healthy vegetation, it is not unreasonable to assume that the soil moisture for the majority of vegetated patches in an irrigated urban neighborhood is maintained around, or above, the critical point during dry periods.

3.2 Influence of long-term soil water representation

The simulations that maintained the soil moisture at the critical point also have a beneficial impact in reducing β at the Baltimore site, and to a much smaller extent for the Lodz site, even though the initial soil moisture after the spin-up simulation was above the critical point for these sites (Fig. 2).

Both the Baltimore and Lodz sites are multi-year datasets and as such, it is not only the initial soil moisture that will impact on overall β, but also the longer term evolution of the soil moisture during the model simulation. Figure 4 (solid lines) shows the initial soil moisture profile (at the end of the spin-up period), the final soil moisture profile at the end of the simulation and soil moisture profiles at the end of each calendar year throughout the model simulation, for each of the four sites with more than 12 months of data (Baltimore, Helsinki, Lodz and Melbourne). By comparing the soil moisture profiles at the same time over consecutive years (i.e., the end of the calendar year), along with the initial and final soil moisture profiles from the model run, it is possible to identify if the modelled soil moisture has a drying or wetting tendency throughout the simulation. For instance, at the Baltimore site the bottom model level soil moisture (which has the long term memory) is consistently drier each year throughout the simulation. The same is also true, but to a lesser extent, for the Lodz site. The Melbourne site has almost no change in bottom layer soil moisture, but benefits from setting the soil moisture to the critical point because all of the soil moisture profiles are much lower than the critical point. For the Helsinki site there is no trend in the bottom layer soil moisture, and hence the soil moisture state is not out of balance. The soil moisture for Helsinki is above the critical point for all of the profiles, which is consistent with there being no impact on β when setting the soil moisture profile to the critical point (Fig. 3).

The drying trends in soil moisture profile over the period of the simulations for both the Baltimore and Lodz sites could result from relatively dry conditions during the observational period compared to the previous years. However, it is more likely that the observational dataset has lower mean precipitation than the WFDEI dataset used for the spin-up of the soil moisture (section 2.4). Hence the spun-up soil moisture is too wet relative to the mean climate of the observational data taken from the study site. So the soil moisture dries during the analysis period when the model is forced by the data from the observational site.
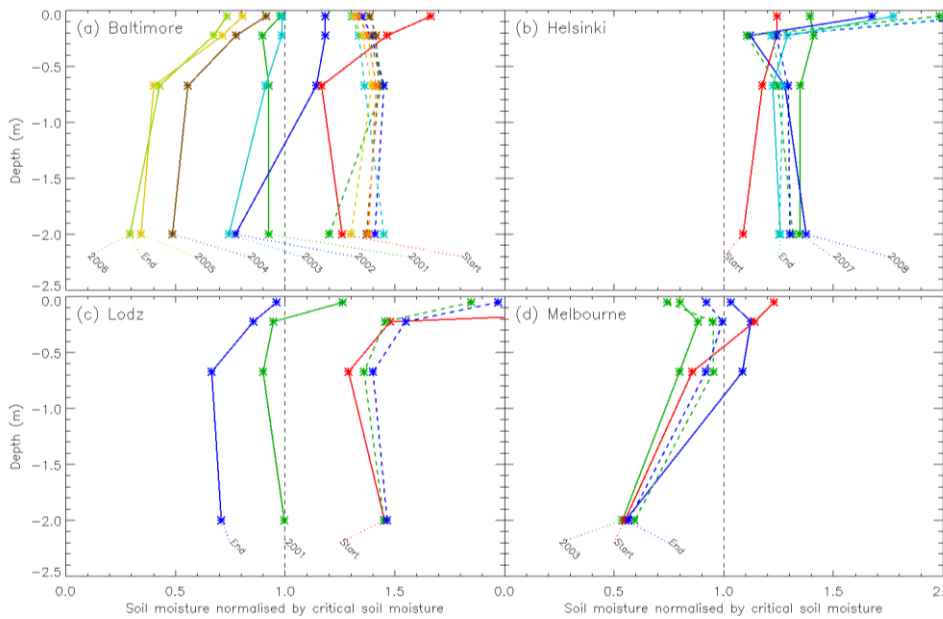
Whilst it is not possible to compare the average precipitation between the observational dataset and that of WFDEI for the spin-up period (because this is the period before the observational data starts), it is possible to compare precipitation during the observational period itself. Figure 5 shows the biases in precipitation for the WFDEI data relative to the observations from the four long term sites. This figure shows clearly that there is more precipitation in the WFDEI dataset for Baltimore than in the observational dataset for the site. For the other three sites, there is less difference between the average precipitation from WFDEI and the observations from the sites, although for Lodz there is slightly more precipitation in WFDEI.

The bias for WFDEI compared to the observational data at the Baltimore site suggests that the precipitation in WFDEI is in error. However, the precipitation data in the observational dataset for Baltimore has not previously been analysed, so the quality of these data is not known. To investigate if the issue is with WFDEI or the observational data at the study site, precipitation data were retrieved from synoptic stations close to the four sites: Baltimore Washington International Airport (39.2° N, 76.7° W), Helsinki/Seutula (60.3° N. 25.0° E), Lodz-Lublinek (51.7° N, 19.4° E) and Melbourne Airport (37.7° S, 144.8° E) (data obtained through NOAA's National Climate Data Center: http://www.ncdc.noaa.gov/). The synoptic reporting stations follow the World Meteorological Organisation (WMO) standards and as such include long term measurements of precipitation.

The distribution of biases between the synoptic data and observational data from the sites (Synop – Obs), and between WFDEI and synoptic data (WFDEI – Synop) are shown in Fig. 5. This shows clearly that for the Baltimore site, the WFDEI precipitation data are in closer agreement with the synoptic data than the observational data from the study site, although the synoptic station may have been included in the data analysis used to create the WFDEI dataset. This suggests that there may be errors in the previously unprocessed precipitation data for the Baltimore site. For the Lodz site, where the precipitation data from the observational site has previously been analysed, the WFDEI dataset is also in better agreement with the synoptic station data, but the differences are much smaller than for the Baltimore site, i.e., the three datasets are in better agreement.

The implications for Baltimore are that the original simulation using the observed precipitation forcing from the site (Fig. 1) had a negative bias in the observations (i.e., too little rainfall). To assess the impact of this, the model was re-run for Baltimore and Lodz with all atmospheric forcing data provided from the WFDEI dataset rather than the observational data from the study site (Fig. 6). All data were used, rather than just the precipitation data from WFDEI, to ensure consistency between the atmospheric data (e.g., to avoid simulating precipitation from WFDEI under clear sky conditions from the observational dataset at the study site). Any issues that arise from forcing the JULES model with data at the atmospheric heights of the WFDEI data have been neglected in this study. Whilst such an assumption may not be valid, there are no other options available for obtaining consistent forcing data at more appropriate heights.

The greater precipitation from the WFDEI dataset maintains the soil moisture profile above the critical point for the Baltimore site and the drying tendency between years is removed (dashed lines in Fig. 4). The removal of the restriction on evapotranspiration from the limitation of soil moisture means that the modeled β is reduced to values that are less than those observed (Fig. 6), which is consistent with many of the other sites in Fig. 3. The drying of the soil moisture profiles between years for the Lodz site is also removed with the WFDEI forcing (dashed lines in Fig. 4), but there is little difference in the resulting β (Fig. 6).

Fig. 4: Initial, final and end of calendar year soil moisture profiles from model integrations at multi-year observational sites. The solid lines show the model profiles when forced with the local observational data. The dashed lines show the model profiles when forced with the WFDEI data. Note Baltimore, Helsinki and Lodz are northern hemisphere sites, whereas Melbourne is southern hemisphere.

The remaining two sites in Fig. 4 (Helsinki and Melbourne) have smaller differences in soil moisture profiles between years from changing the data used for the forcing of JULES (cf., solid and dashed lines in Fig. 4). This is consistent with WFDEI data and the observations from the study site having similar precipitation averages (Fig. 5).

Fig. 5: Distribution (inter-quartile range, median and 10th and 90th percentiles, as per Fig. 1) of bias in precipitation between WFDEI and observations at the study site, synoptic data and observations at the study site, and WFDEI and synoptic data, for the multi-year sites.

3.3 Influence of bare soil surfaces

Whilst additional anthropogenically applied water might be responsible for maintaining vegetation transpiration rates at many of the sites, it is unlikely that unmanaged or bare soil areas are also irrigated. However, in the JULES model the different surface types share the same underlying soil. Hence setting the soil moisture profile to the critical point during the simulation will also unrealistically increase the bare soil evaporation and provide an infinite reservoir of water as conservation of mass is no longer constrained. As both the Ouagadougo and Tucson sites had a substantial fraction of bare soil or unmanaged land cover, they could be affected by this model limitation.

To investigate the impact on β, Q_H and Q_E were determined by the weighted average values from the individual surface types taken from two simulations. For vegetation surfaces, Q_H and Q_E were taken from the JULES simulation with the soil moisture set to the critical point, whilst for all other surfaces Q_H and Q_E were taken from the original default JULES
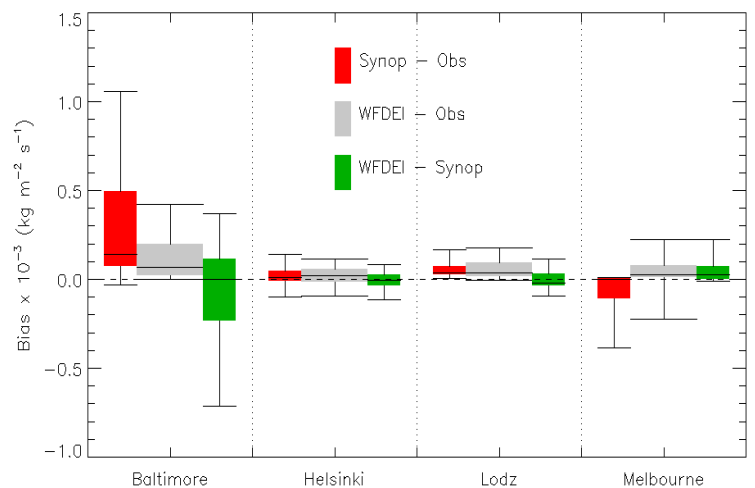
simulation. As there are no atmospheric feedbacks in these JULES simulations, this is equivalent to irrigating only the vegetation part of the land cover.

The resulting β for the Tucson and Ouagadougo sites are shown in Figure 6. The higher water availability for bare soil evaporation from the simulation with the soil moisture set to the critical point gave values of β that were substantially lower than those observed (Fig. 6). However, irrigating only the vegetated area reduced the unrealistically high β values from the original simulation for these sites (Fig. 6), but does not lead to such low values. Indeed, for Tucson the resulting β is in good agreement with the observed values, whist for Ouagadoudo the modelled β is higher than observed, but within the range of the observations.
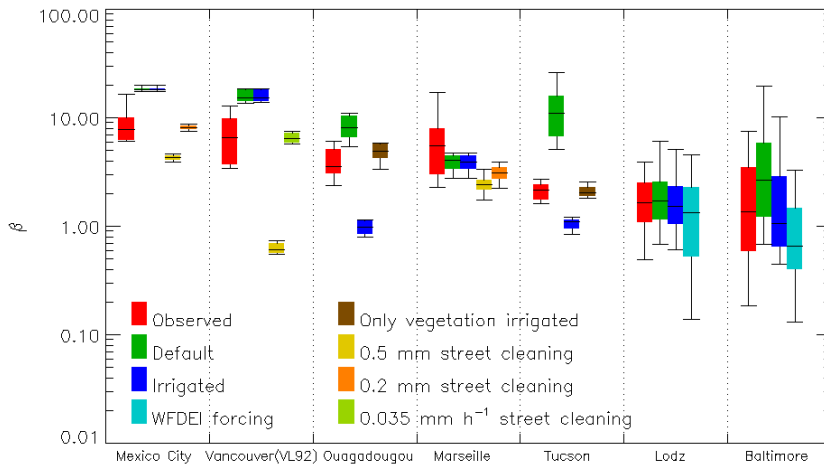

Fig. 6: as for Fig.1, Observed and JULES model runs: initial/Default and with anthropogenic moisture added in various ways (Irrigated – soil moisture fixed at the critical point; only vegetation irrigated – soil moisture held at critical point for vegetated land cover only; 0.5 mm street cleaning – artificial precipitation added to forcing in the morning amounting to a total of 0.5 mm; 0.2 mm street cleaning – artificial precipitation added to forcing in the morning amounting to a total of 0.2 mm; 0.035 mm h^{-1} street cleaning – artificial precipitation added to forcing each hour between 09:00 – 17:00 amounting to a total of 0.035 mm every hour) and using WFDEI forcing (WFDEI precipitation instead of observations at the study site). See text for further discussion. Sites are organised by increasing plan area fraction vegetated (see Table 2 for values).

3.4 Influence of street cleaning

The modelled β for the Mexico City and Vancouver (VL92) sites are substantially larger than the observed values (Fig. 1). Setting the soil moisture to the critical point has no impact on modelled β (Fig. 3) because the fraction of vegetation and bare soil within the footprint is small for both sites (1% and 2% for Mexico City and 5% and 0% for Vancouver (VL92)). Hence the available water for Q_E must come from a different source to the vegetation or bare soil surfaces.

At the Mexico City site, there was daily cleaning of the streets in the morning in preparation for the market (Oke et al., 1999). To understand if this source of water can explain a lower β in the observations at Mexico City, artificial precipitation was added to the forcing dataset between the local hours of 07:00 and 08:00 each day. In addition, to ensure that the resulting water could only be retained on the street part of the urban surface and not the roofs, the water holding capacity of the roofs was set to zero. The amount of artificial precipitation each day was set to the maximum water holding capacity of the street, which is 0.5 mm in the default parameter settings of JULES (Best et al., 2011). Hence this water reservoir within the street was set to its maximum value at this time, for each day of the simulation. In this scenario, the resulting modelled β is greatly reduced and results in values that are substantially below those observed (Fig. 6).

Information of the actual residual water that remained after the street cleaning process is not available from the field study and so it is not clear if the correct amount of water was added to the street surface within the model. A sensitivity study, by varying the amount of artificial daily precipitation, shows that the optimal value of water held within the street to give the same average β as that observed was around 0.2 mm. (Fig. 6). Hence it is feasible, and perhaps likely, that the source of water from street cleaning was responsible in reducing β to that observed.

Street cleaning was also undertaken at the Marseille site during mid-morning after the market (Grimmond et al., 2004). The same artificial total precipitation required to fill the maximum water holding capacity of the street (0.5 mm) and the optimal value obtained for Mexico City (0.2 mm) were applied to the Marseille site, expect that the artificial precipitation was added between 10:00 and 11:00 each day. In this case the additional source of water has less of an impact because there is already a Q_E from the irrigated vegetation faction. However, β is reduced when the water from street cleaning is added (Fig. 6), with 0.2 mm of water resulting in a median that is in better agreement with the observations than 0.5 mm, as for the Mexico City site.

3.5 Influence of advective fluxes

No additional source of water at the surface was documented during the observational period for the Vancouver (VL92) site. Indeed, during this period Vancouver was experiencing drought conditions and was under an irrigation ban (Grimmond and Oke, 2002). As such, the mid-day Q_E observed are small compared to the net all-wave radiation or the downward component of the short-wave radiation (Fig. 7). Small Q_E values typically have larger measurements error.

This can be associated with measurements of low turbulence conditions by the sonic anemometer and/or low moisture availability measurements by the gas analyser. Conditions of dew formation also increase measurement errors. The lack of energy balance closure in observational datasets is frequently attributed to underestimation of the turbulent heat fluxes and a hysteresis effect in the storage heat flux (e.g., Leuning et al., 2012). In the current situation any corrections would proportionally increase Q_E, and thus maintain or reduce β. So it is unlikely that the differences between the modelled and observed β values can be explained through observational errors.
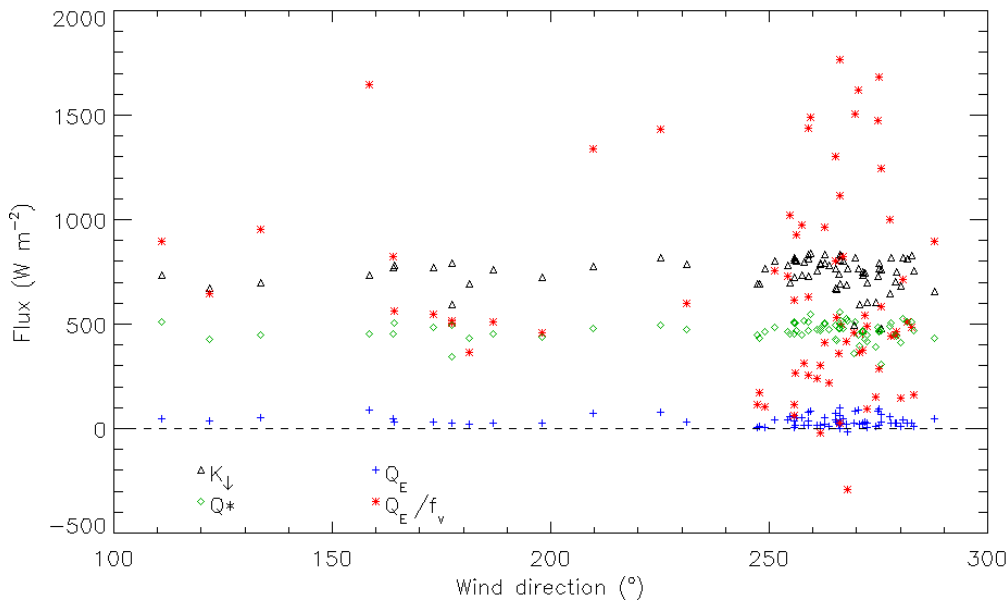

Fig. 7: Mid-day (10:00 – 14:00 local solar time) incoming solar radiation (K↓), net all-wave radiation (Q*), latent heat flux density (Q_E) and latent heat flux density scaled by fraction of vegetation land cover within observational footprint (Q_E/f_v), against wind direction for the Vancouver (VL92) site.

As there was no precipitation during the observational period, the only water store at the land surface would be through the soil moisture. Since there was no bare soil surface within the source area of the observed fluxes, this implies that the only possible moisture source from the surface would be through transpiration from the vegetation. Fig. 2 shows that the initial soil moisture profile for the Vancouver (VL92) site after the model spin-up was such that there was no soil moisture stress on the vegetation, even though the site was actually in drought conditions. So the underestimation of Q_E, and hence high β, from the model cannot be explained by the initial conditions. This is also confirmed by the run with soil moisture held at the critical point, since this run does not impact on modelled β (Fig. 3).

If the observed mid-day values of Q_E at Vancouver (VL92) are scaled by the vegetation fraction, f_v (i.e., assuming that the water vapour can only originate from transpiration from the vegetation fraction of the land cover), then the resulting Q_E from the vegetation is larger than the observed net all-wave radiation (Fig. 7), although for a rigorous comparison the net all-wave radiation should also be adjusted to reflect the value over just the vegetation. However, the rescaled evaporation (Q_E/ f_v) is larger than the downward component of the shortwave radiation at times, which needs no such adjustment for vegetation fraction. Hence it is very unlikely that Q_E observed at the Vancouver (VL92) site originated from soil moisture through transpiration within the turbulent source area of the eddy-covariance observations on the tower.

As this was an industrial site, although there was no street cleaning documented, it is possible that there were some equivalent activities that could lead to a source of water on impervious surfaces. As such, a simulation with sufficient artificial total precipitation to fill the maximum water holding capacity of the street (0.5 mm) was applied for each hour between the working hours of 09:00 and 17:00 on each day. The addition of this water each hour provides a source reservoir that is large enough to reduce β to values far less than observed (Fig. 6). However, a sensitivity study shows that an amount of 0.035 mm each hour gives a modelled median of β that is close to that observed (Fig. 6). Hence it requires only a small amount of water to be added each hour to explain the observed β, so it is possible that such a source of water is responsible for the observed evaporation.

An alternative explanation is that the moisture originates from the advective flux at atmospheric levels below the height of the eddy covariance system. Indeed, the wind direction around mid-day for most of the observational period was from the direction of False Creek, an inlet of the Pacific Ocean located 600 m to 1 km upwind of the tower. A relatively warm and dry surface such as that within the observational footprint could give the buoyancy required to lift the advected vapour flux at low levels, hence leading to an observed mid-day average Q_E of 36 W m^{-2} at the site.

3.6 Influence of a garden irrigation ban

The Vancouver (VS92) site is the only site where the model substantially underestimates the observed β (Fig. 3). The observational period for this site coincided with the Vancouver (VL92) site, so was also experiencing drought conditions with an irrigation ban. However, the initial soil moisture profile for the model derived from the spin-up has a soil moisture profile that is above the critical point, and hence the vegetation in the model is not soil moisture stressed

(Fig. 2). This implies that there was too much precipitation in the forcing data from the WFDEI dataset during the spin-up period, especially during the period immediately prior to the start of the observations at the study site.

Observations for the Vancouver (VS92) dataset were taken over 56 days, during which there was no precipitation in either the observational dataset or the WFDEI dataset. Therefore it is not possible to make conclusions about any biases that there could be in the WFDEI dataset compared to the observations at the study site. In addition, the complex topography of the Vancouver area and its coastal location results in large precipitation gradients across the city (Oke and Hay, 1998). As such, comparing the WFDEI dataset to a synoptic station would not necessarily result in any conclusions about precipitation biases compared to the observations at the study site. Moreover, the WFDEI dataset has a resolution of 0.5° and as such can not be expected to give accurate precipitation values for specific parts in a region of such topographic heterogeneity.

The WFDEI dataset has two precipitation datasets based upon monthly climatologies from either GCPC or CRU (section 2.3). In this study we have used the values from the GCPC data, but both climatologies are based upon a similar global precipitation gauge network. The number of gauges used for the climatology has a much lower density in the Vancouver (Canada) region compared to the coastal regions just to the south in the USA (see Schneider et al., 2013, Fig. 5). Also, New et al. (2000, their Fig. 1) show that the rain gauge density used for the CRU climatology decreased substantially between 1981 and 1995. Hence it is quite likely that with the heterogeneous nature of precipitation around Vancouver and the rain gauge density during the period of the observational campaign could have resulted in a lower quality precipitation product for this site compared to other regions that have higher gauge densities. Thus the 10 year spin-up for both Vancouver sites (VL92 and VS92) could be impacted.

Irrigation restrictions were also enforced during the summer at the Melbourne site. However, unlike the complete ban at Vancouver (VS92 and VL92), at Melbourne this involved no watering of lawns, whilst for trees and other vegetation automatic sprinkler systems were limited to the hours between 23:00 and 06:00, and manual sprinkler systems limited to the hours between 05:00 and 08:00 and 20:00 and 23:00. In addition, although the times during which irrigation could be applied were limited, the amount of water was not.

Calculating an average β for both the summer and winter at the Melbourne site shows that although β is slightly reduced in the winter, there is no impact on the ability of the model to simulate the observed values if it is assumed that the vegetation is sufficiently irrigated (not shown). The summer values for both observed and modelled β are similar to the overall results. Hence the partial irrigation ban for the Melbourne site has little impact on the overall β compared to the complete ban at the Vancouver (VS92) site.

4. Conclusions

The initial soil moisture conditions have been shown previously to be critical for modelling sensible and latent heat fluxes in urban environments (Best and Grimmond, 2015a). In this study, initialising soil moisture with saturated conditions prior to a 10 year spin-up is shown to produce a soil moisture profile that is consistent with the model physics whilst enabling a realistic simulation, as long as there are no additional anthropogenic water sources such as irrigation. Hence we recommend this for future studies when soil moisture profile observations are unavailable.

In addition, the WFDEI dataset is demonstrated, in general, to provide good quality forcing data that can be used with this spin-up strategy. Whilst the quality of the precipitation data within the WFDEI dataset can vary depending upon the rain gauge density used to create monthly climatologies such as GPCC and CRU, it was of sufficient quality for most of the sites considered in this study. Hence we also conclude that by using the WFDEI data and the 10 year spin-up strategy, it should be possible to initialise a LSM (including ULSM) at any site, as long as consideration is given to the density of rain gauges used for the monthly precipitation climatology, in addition to anthropogenic water sources.

In a summary of the results from PILPS-Urban, Best and Grimmond (2015a) concluded that the important processes in the urban environment were the bulk reflection of the downward shortwave radiation, the influence of the urban morphology on the longwave radiation fluxes and the vegetation processes for the distribution of the sensible and latent heat fluxes. This study has focused on the ability of JULES to simulate β across 22 observational datasets, i.e., exploration of the model's ability to partition surface energy between the sensible and latent heat fluxes. Hence the third physical process identified by Best and Grimmond (2015a) is addressed. However, a good simulation of β does not necessarily imply that the model gives accurate values of Q_H and Q_E separately, which are also influenced by the radiative processes.

The results from the model show that at sites where the transpiration from vegetation is not restricted by limited soil moisture the model can reproduce observed β, whilst for the sites with limited soil moisture the model overestimates β compared to the observations. However, if we make the assumption that urban sites are irrigated to ensure that vegetation is not soil moisture stressed (i.e., urban residents maintain 'healthy' gardens and parks), then the model is in good agreement with observed β at these sites as well. The one exception, the Vancouver (VS92) site, was known to be

in drought conditions with an irrigation ban in force. Hence we conclude that when modelling vegetation within urban environments it should be assumed that the vegetation is not soil moisture stressed, unless it is known to be a dry period with an irrigation ban in place. Given these assumptions, the JULES model is able to represent the observed urban β over the range of plan area vegetation fractions considered in this study (Fig. 8a).

The possibility of an irrigation ban within urban environments makes the modelling of urban vegetation complex, but important. The availability of soil moisture for transpiration is not a physical condition as it is for the rural environment, but becomes a combination of physical and social conditions. Factors such as population density (i.e., water demand), wealth (e.g., artificial water storage applications), national infrastructure (i.e., transport of water) and stakeholder requirements (e.g., city dweller water use versus agricultural irrigation) may all influence the political decision making with regards to an irrigation ban. For instance, compare the different urban water use practices and water availability in the climates of Ouagadougou (Offerle et al., 2005b), Marseille (Grimmond et al., 2004), Vancouver and Chicago (Grimmond and Oke, 1999), and Arcadia and San Gabriel (Grimmond et al., 1996). Hence we conclude further studies are needed to investigate the implementation of irrigation bans and their impact on the surface energy and water balance for urban areas.

Irrigation of vegetation is not the only anthropogenic moisture source that can influence the turbulent fluxes of heat and moisture within the urban environment. This work has shown that activities such as street cleaning can provide a source of water that can moderately increase Q_E. Hence all possible sources of anthropogenic water are important and need to be represented within an urban land surface model. Furthermore, the impact of such anthropogenic water injections suggests that they are at least as important as the anthropogenic heat flux density on the terms in the surface energy balance for urban areas.
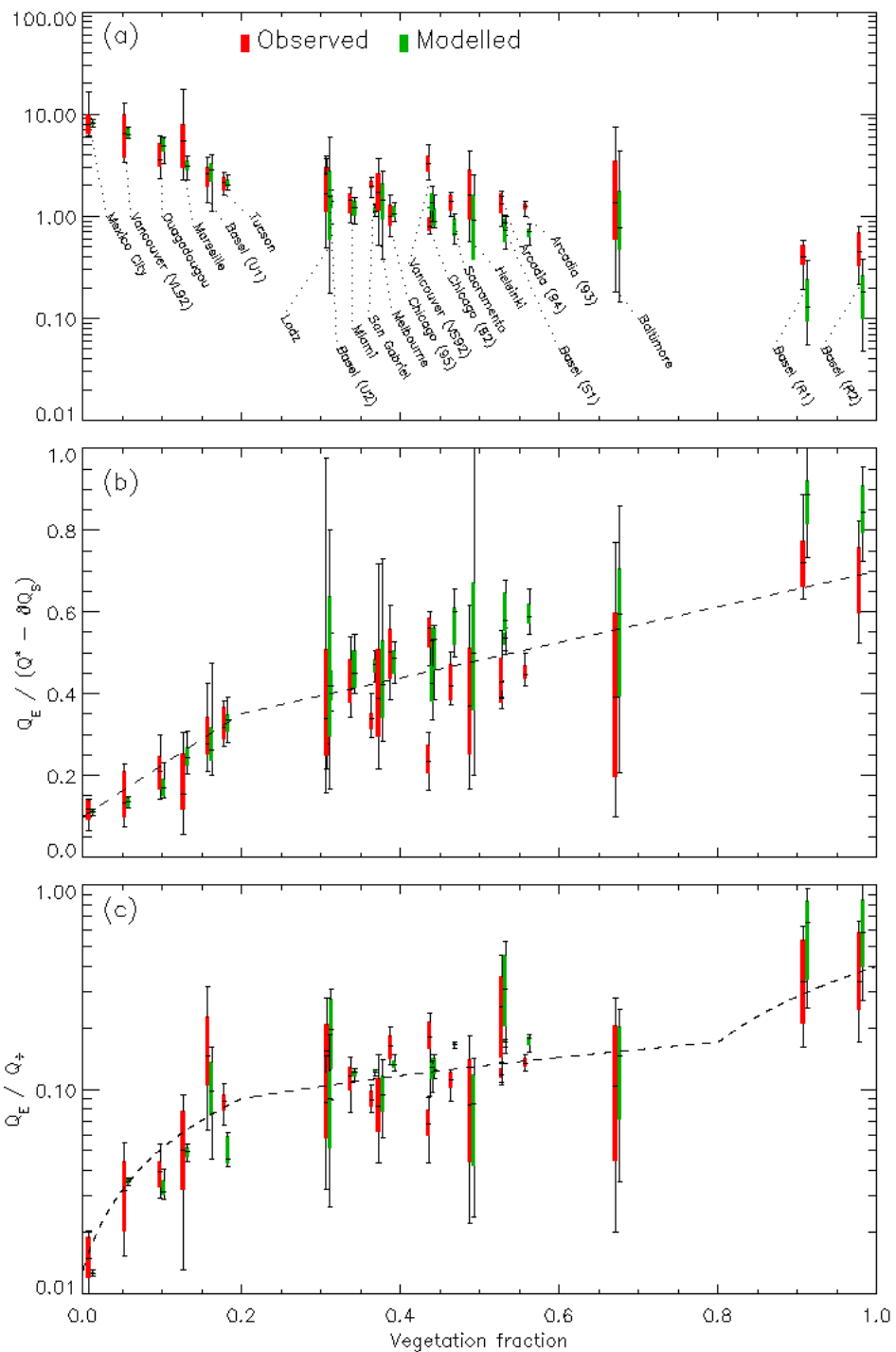
For well irrigated vegetation, there is little change in β for sites with vegetation cover between 30% and 70% (Fig. 8a). Whilst there is some day to day variability at the sites, the average β is typically in the range of 1-2. The two rural sites near Basel with almost total vegetation cover (R1, R2) have β values less than one, which is typical for rural locations. However, as the vegetation fraction decreases below 20%, β increases substantially with a maximum value of around eight for the most densely built up urban site studied here (Mexico City). However, for this site β was reduced due to being controlled by water availability from street cleaning. Also, for the second most impervious site (Vancouver (VL92)), the observations may have been influenced by water added to the surface in a similar manner to street cleaning, or atmospheric advection of moisture into the source area at levels below the height of the observations. As such, it is possible that without these additional sources of moisture, β could be as large as 20 for urban sites with little vegetation during summertime. However, Offerle et al. (2006b) suggested that sparse vegetation may well be exposed to higher vapour pressure deficits and higher temperatures, whilst isolated trees are exposed to higher Photosynthetic Active Radiation (PAR), which could increase transpiration. Also, Meier and Scherer (2012) concluded that trees surrounded by a high fraction of impervious surfaces showed consistently higher canopy temperatures. In addition, we have made no attempt to distinguish between native and non-native vegetation. High latitude, mid-latitude, semi arid and tropical vegetation all have different characteristics which could influence the results for sparse vegetation cover. Hence additional observational studies are required for urban environments with sparse vegetation and no additional anthropogenic water injections, to determine the behavior of vegetation in such environments.

If we consider how Q_E varies with vegetation fraction, we find that as a proportion of the available energy at the surface, there is a step change around vegetation fractions of 20-30% (Fig. 8b). This step change is also seen when scaling Q_E by the incoming all-wave radiation (Fig. 8c). This result agrees with Loridan and Grimmond (2012a) who found such a step change in the scaled Q_E against their active vegetation index. Furthermore, when scaled by the incoming all-wave radiation, there is also a step change in Q_E with almost total vegetation cover (70-90%, Fig 8c), or little built area cover, although this step change is not seen in Q_E as a proportion of the available energy at the surface. This suggests that there could be a step change in the net heat storage flux density for small built fractions, as confirmed by the results of Loridan and Grimmond (2012a) who showed a step change in the storage heat density for changes in active built index. Hence we conclude that the sensitivity of Q_E, and hence the Q_H through the available energy at the surface, is greatly increased when there is little vegetation cover, whilst the sensitivity of the heat storage is greatly increased when there is little built area cover.

The results from this study suggest that an urban land surface model, such as JULES, can reproduce the observed β values of urban sites. However, the sensitivity of the urban energy balance at sites with low fractions of vegetation land cover, or low fractions of built area, suggests that further studies are required for urban environments with less than 30% vegetation cover, and less than 30% built area cover. This can only be achieved if there are future observational campaigns for such environments, or observational data are analysed according to wind sectors that have differing plan area vegetation fractions. Future observational campaigns need to be long term in order to sample a range of synoptic and climatic extremes, so that the nature of the variability and sequencing can be evaluated for their impacts on the surface fluxes.

Fig. 8: Mid-day (10:00 – 14:00 local solar time) variability of observed and modelled (a) Bowen ratio (β), (b) latent heat scaled by available energy (net all-wave radiation, Q*, minus the net storage heat flux, ΔQs, ignoring the anthropogenic heat flux, QF) and (c) latent heat flux scaled by incoming all-wave radiation (Q↓), shown with the inter-quartile range (box), median (-) and 10th and 90th percentiles (whiskers). Linear dashed lines have no significance and are purely a visual guide.

References

Best, M. J., 2005: Representing urban areas within operational numerical weather prediction models. *Boundary-Layer Meteorol,* **114**, 91–109.

Best, M.J., C. S. B Grimmond, 2013: Analysis of the seasonal cycle within the first international urban land surface model comparison. *Boundary-Layer Meteorol,* **146**, 421-446, doi: 10.1007/s10546-012-9769-7

Best, M.J., C. S. B. Grimmond, 2014: Importance of initial state and atmospheric conditions for urban land surface models performance. *Urban Climate,* **10**, 387-406, doi:10.1016/j.uclim.2013.10.006

Best, M.J., C. S. B. Grimmond, 2015a: Key conclusions of the first international urban land surface model comparison. *Bulletin of the American Meteorol. Soc.,* **96**, 805-819, doi:http://dx.doi.org/10.1175/BAMS-D-14-00122.1

Best, M.J., C. S. B. Grimmond, 2015b: Investigation of the impact of anthropogenic heat flux within an urban land surface model and PILPS-urban. *Theor. Appl. Cliatol.*, doi:10.1007/s00704-015-1554-3

Best, M. J., C. S. B Grimmond, M. G. Villani, 2006: Evaluation of the urban tile in MOSES using surface energy balance observations. *Boundary- Layer Meteorol,* **118**, 503–525.

Best, M. J., M Pryor, D. B. Clark, G. G. Rooney, R. H. L. Essery, C. B. Ménard, J. M. Edwards, M. A. Hendry, A. Porson , N. Gedney, L. M. Mercado, S. Sitch, E. Blyth, O. Boucher, P. M. Cox, C. S. B. Grimmond, R. J. Harding, 2011: The Joint UK Land Environment Simulator (JULES), Model description – Part 1: Energy and water fluxes. *Geosci Model Dev,* **4**, 677-699

Best, M. J., G. Abramowitz, H. R. Johnson, A. J. Pitman, G. Balsamo, A. Boone, M. Cuntz, B. Decharme, P. A. Dirmeyer, J. Dong, M. Ek, Z. Guo, V. Haverd, B. J. J van den Hurk, G. S. Nearing, B. Pak, C. Peters-Lidard, J. A. Santanello Jr., L. Stevens, N. Vuichard, 2015: The plumbing of land surface models: benchmarking model performance. *J. Hydrometeorol.,* **16**, 1425-1442, doi:10.1175/JHM-D-14-0158.1.

Christen, A., R. Vogt, 2004: Energy and radiation balance of a central European city. *Int. J. Climatol.,* **24**, 1395-1421.

Collatz, G. J., J. T. Ball, C. Grivet, J. A. Berry, 1991: Physical and environmental regulation of stomatal conductance, photosynthesis and transpiration: a model that includes a laminar boundary layer. *Agric. Forest Meteorol.*, **54**, 107-136.

Collatz, G. J., M. Ribas-Carbo, J. A. Berry, 1992: Coupled phytosynthesis-stomatal conductance model for leaves of C4 plants. *Aust. J. Plant Physiol.*, **19**, 519-538.Coutts, A. M., J. Beringer, N. J. Tapper, 2007a: Characteristics influencing the variability of urban CO2 fluxes in Melbourne, Australia. *Atmos Environ*, **41**, 51–62.

Coutts, A. M., J. Beringer, N. J. Tapper, 2007b: Impact of increasing urban density on local climate: spatial and temporal variations in the surface energy balance in Melbourne, Australia. *J Appl Meteorol, 47*, 477–493.

Crawford, B., C. S. B. Grimmond, A. Christen, 2011: Five years of carbon dioxide fluxes measurements in a highly vegetated suburban area. *Atmos. Environ., 45*, 895-905.

Dee, D. P., S. M. Uppala, A. J. Simmons, P. Berrisford, P. Poli, S. Kobayashi, U. Andrae, M. A. Balmaseda, G. Balsamo, P. Bauer, P. Bechtold, A. C. M. Beljarrs, L. van de Berg, J. Bidlot, N. Bormann, C. Delsol, R. Dragani, M. Fuentes, A. J. Geer, L. Haimberger, S. B. Healy, H. Hersbach, E. V. Hólm, L. Isaksen, P. Kållberg, M. Köhler, M. Matricardi, A. P. McNally, B. M. Monge-Sanz, J.-J. Morcrette, B.-K. Park, C. Peubey, P. de Rosnay, C. Tavolato, J.-N. Thépaut, F. Vitart, 2011: The ERA-Interim reanalysis: Configuration and performance of the data assimilation system, *Q. J. R. Meteorol. Soc., 137*, 553–597

Dupont, S., P. G. Mestayer, 2006: Parameterisation of the urban energy budget with the submesoscale soil model. *J Appl Meteorol Climatol 45*, 1744–1765.

Fortuniak, K., 2003: A slab surface energy balance model (SUEB) and its application to the study on the role of roughness length in forming an urban heat island. *Acta Universitatis Wratislaviensis, 2542*, 368–377.

Grimmond, C. S., B., A. Christen, 2012: Flux measurements in urban ecosystems. *FluxLetter: The Newsletter of Fluxnet, 5*, 1-8.

Grimmond, C. S. B. , T. R. Oke, 1986: Urban water balance. 2. Results from a suburb of Vancouver, British Columbia. *Water Res. Research, 22*, 1404-1412.

Grimmond, C. S. B. , T. R. Oke, 1995: Comparison of heat fluxes from summertime observations in the suburbs of four North American cities. *J Appl Meteorol, 34*, 873-889.

Grimmond, C. S. B. , T. R. Oke, 1999: Heat storage in urban areas: local-scale observations and evaluation of a simple model. *J Appl Meteorol, 38*, 922-940.

Grimmond, C. S. B., T. R. Oke, 2002: Turbulent heat fluxes in urban areas: observations and local-scale urban meteorological parameterization scheme (LUMPS). *J Appl Meteorol, 41*, 792–810.

Grimmond, C. S. B. , T. R. Oke, H. A. Cleugh, 1993: The role of 'rural' in comparisons of observed suburban-rural flux differences. *Int. Assoc. Hydrolog. Sci. Publ., 212*, 165-174.

Grimmond, C. S. B. , C. Souch, M. D. Hubble, 1996: Influence of tree cover on summertime surface energy balance fluxes, San Gabriel Valley, Los Angeles. *Clim Res, 6*, 45-57.

Grimmond, C. S. B., J. A. Salmond, T. R. Oke, B. Offerle, A. Lemonsu, 2004: Flux and turbulence measurements at a densely built-up site in Marseille: heat, mass (water and carbon dioxide), and momentum. *J Geophys Res, 109*, D24101, doi:10.1029/2004JD004936.

Grimmond, C. S. B., M. Blackett, M. J. Best, J.-J. Baik, S. E. Belcher, J. Beringer, S. I. Bohnenstengel, I. Calmet, F. Chen, A. Coutts, A. Dandou, K. Fortuniak, M. L. Gouvea , R. Hamdi, M. Hendry, M. Kanda, T. Kawai, Y. Kawamoto, H. Kondo, E. S. Krayenhoff, S.-H. Lee, T. Loridan, A. Martilli, V. Masson, S. Miao, K. Oleson, R. Ooka, G. Pigeon, A. Porson, Y.-H. Ryu, F. Salamanca, G.-J. Steeneveld, M. Trombou, J. Voogt, D. Young, N. Zhang, 2011): Initial results from phase 2 of the international urban energy balance model comparison, *Int. J. Climatol., 30*, 244-272, doi:10.1002/joc.2227.

Harris, I., P. D. Jones, T. J. Osborn, and D. H. Lister, 2013: Updated high-resolution grids of monthly climatic observations - The CRU TS3.10 dataset. *Int. J. Climatol., 34*, 623–642, doi:10.1002/joc.3711.

Järvi, L., C. S. B. Grimmond, M. Taka, A. Nordbo, H. Setälä, I. B. Strachan, 2014: Development of the surface urban energy and water balance scheme (SUEWS) for cold climate cities. *Geosci. Model Dev., 7*, 1691-1711, doi:10.5194/gmd-7-1691-2014.

Kawai, T., M. K. Ridwan, M. Kanda, 2009: Evaluation of the simple urban energy balance model using 1-yr flux observations at two cities. *J. Appl. Meteorol. Climatol., 48*, 693–715.

King, T., C. S. B. Grimmond, 1997: Transfer mechanisms over an urban surface for water vapor, sensible heat, and momentum. In Preprints, 12th Conf. on Boundary layers and turbulence, Vancouver, BC, Canada. Am. Meteorol. Soc: Boston, M.A, pp 455-456

Kondo, H., Y. Genchi, Y. Kikegawa, Y. Ohashi, H. Yoshikado, H. Komiyama, 2005: Development of a multi-layer urban canopy model for the analysis of energy consumption in a big city: structure of the urban canopy model and its basic performance. *Boundary-Layer Meteorol, 116*, 395–421.

Krayenhoff, E. S., J. A. Voogt, 2007: A microscale three-dimensional urban energy balance model for studying surface temperatures. *Boundary- Layer Meteorol, 123*, 433–461.

Lee, S.-H., S.-U. Park, 2008: A vegetated urban canopy model for meteorological and environmental modelling. *Boundary-Layer Meteorol., 126*, 73–102.

Leuning, R., E. van Gorsel, W. J. Massman, P. R. Isacc, 2012: Reflections on the surface energy imbalance problem. *Agricultural and Forest Meteorol., 156*, 65-74, doi:10.1016/j.agrformet.2011.12.002.

Loridan, T., C. S. B. Grimmond, 2012a: Characterization of energy flux partitioning in urban environments: links with surface seasonal properties. *J. Appl. Meteorol. Climatol., 51*, 219-241, doi:10.1175/JAMC-D-11-038.1.

Loridan, T., C. S. B. Grimmond, 2012b: Multi-site evaluation of an urban land-surface model: intra-urban heterogeneity, seasonality and parameter complexity requirements. *Q. J. R. Meteorol. Soc., 138*, 1094-1113, doi:10.1002/qj.963.

Loridan, T., C. S B. Grimmond, B. D. Offerle, D. T. Young, T. E. L. Smith, L. Järvi, F. Lindberg, 2011: Local-scale Urban Meteorological Parameterization Scheme (LUMPS): Longwave radiation parameterization and seasonality-related developments. *J. Appl. Meteorol. Climatol., 50*, 185-202, doi:10.1175/2010JAMC2474.1

Martilli, A., A. Clappier, M. W. Rotach, 2002: An urban surface exchange parameterisation for mesoscale models. *Boundary-Layer Meteorol., 10*, 261–304.

Masson, V., 2000: A physically-based scheme for the urban energy budget in atmospheric models. *Boundary-Layer Meteorol, 41*, 1011–1026.

Meier, F., D. Scherer, 2012: Spatial and temporal variability of urban tree canopy temperature during summer 2010 in Berlin, Germany. *Theoretical and Applied Climatol., 110*, 373-384, doi: 10.1007/s00704-012-0631-0.

Monin, A. S., A. M. Obukhov, 1954: Basic regularity in turbulent mixing in the surface layer of the atmosphere. *Moscow, Ak. Nauk. Geof. Inst., 24*, 163-187.

New, M., M. Hulme, P. Jones, 1999: Representing twentieth-century space–time climate variability. Part I: Development of a 1961–90 mean monthly terrestrial climatology. *J. Climate, 12*, 829–856.

New, M., M. Hulme, P. Jones, 2000: Representing twentieth-century space–time climate variability. Part II: Development of 1901–96 monthly grids of terrestrial surface climate. *J. Climate*, **13**, 2217–2238.

Newton, T., 1999: Energy balance fluxes in a subtropical city: Miami, FL. M.S. thesis, Dept. of Geography, University of British Columbia, Vancouver, BC, Canada, 140 pp.

Newton, T., T. R. Oke, C. S. B. Grimmond, M. Roth, 2007: The suburban energy balance in Miami, Florida. *Geografiska Annaler Series A – Phys Geogr.*, **89A**, 331-347.

Offerle, B., C. S. B. Grimmond, K. Fortuniak, 2005a: Heat storage and anthropogenic heat flux in relation to the energy balance of a central European city centre. *International Journal of Climatology,* **25**, 1405-1491.

Offerle, B., P. Jonsson, I. Eliasson, C. S. B. Grimmond, 2005b: Urban modification of the surface energy balance in the West African Sahel: Ouagadougou, Burkina Faso. *J Clim.,* **18**, 3983-3995.

Offerle, B., C. S. B. Grimmond, K. Fortuniak, K. Kłysik, T. R. Oke, 2006a: Temporal variations in heat fluxes over a central European city centre. *Theorectical and Applied Climatol.,* **84**, 103-115.

Offerle, B., C. S. B. Grimmond, K. Fortuniak, W. Pawlak, 2006b: Intraurban differences of surface energy fluxes in a central European city. *J. Appl. Meteorol. Climatol.,* **45**, 125-136.

Oke, T. R., J. E. Hay, 1998: The climate of Vancouver. 2nd Edition, BC Geographical Series, No. 50, Vancouver, 84 pp, ISBN 919478 74 3.

Oke, T.R., A. Spronken-Smith, E. Jauregui, C. S. B. Grimmond, 1999: The energy balance of central Mexico City during the dry season. *Atmos Environ.,* **33**, 3919-3930.

Oleson, K. W., G. B. Bonan, J. Feddema, M. Vertenstein, C. S. B. Grimmond, 2008a: An urban parameterization for a global climate model: 1. Formulation and evaluation for two cities. *J Appl Meteorol Climatol.,* **47**, 1038–1060.

Pawlak, W., K. Fortuniak, M. Siedlecki, 2011: Carbon dioxide flux in the centre of Łódź, Poland – analysis of a 2-year eddy covariance measurement data set. *Int. J. Climatol.*, **31**, 232-243, doi:10.1002/joc.2247

Porson, A., P.A. Clark, I. N. Harman, M. J. Best, S. E. Belcher, 2010: Implementation of a new urban scheme in the MetUM. Part I: Description and idealized simulations. *Q. J. R. Meteorol. Soc.,* **136**, 1514-1529.

Ryu, Y. –H., J. –J. Baik, S. –H. Lee, 2011: A new single layer urban canopy model for use in mesoscale atmospheric models. *J. Appl. Meteorol. Climatol.*, **50**, 1773-1794, doi:10.1175/2011JAMC2665.1.

Schneider, U., A. Becker, P. Finger, A. Meyer-Christoffer, M. Ziese, B. Rudolf, 2013: GPCC's new land surface precipitation climatology based on quality-controlled in situ data and its role in quantifying the global water cycle. *Theor. Appl. Climatol.,* **115**, 15-40, doi: 10.1007/s00704-013-0860-x

Sheng, J., F. Zwiers, 1998: An improved scheme for time-dependent boundary conditions in atmospheric general circulation models. *Climate Dynamics,* **14**, 609-613.

Stewart, I. D., T. R. Oke, 2012: Local Climate Zones for Urban Temperature Studies. *Bulletin of the American Meteorol. Soc.*, **93 (12)**, 1879–1900.

Vesala, T., L. Järvi, S. Launiainen, A. Sogachev, Ü. Rannik, I. Mammarella, E. Siivola, P. Keronen, J. Rinne, A. Riikonen, E. Nikinmaa, 2008: *Tellus*, **60B**, 188-199.

Voogt, J. A., C. S. B. Grimmond, 2000: Modeling surface sensible heat flux using surface radiative temperatures in a simple urban area*. J Appl Meteorol.*, **39**, 1679–1699.

Weedon, G. P., S. Gomes, P. Viterbo, W. J. Shuttleworth, E. Blyth, H. Österle, J. C. Adam, N. Bellouin, O. Boucher, M. Best, 2011: Creation of the WATCH Forcing Data and its use to assess global and regional reference crop evaporation over land during the twentieth century. *J. Hydrometeorol.*, **12**, 823-848, doi:10.1175/2011JHM1369.1

Weedon, G.P., G. Balsamo, N. Bellouin, S. Gomes, M. J. Best, P. Viterbo, 2014: The WFDEI meteorological forcing data set: WATCH Forcing Data methodology applied to ERA-Interim reanalysis data, *Water Resour. Res.,* **50**, doi:10.1002/2014WR015638